A General Method to Determine the Optimal Profile of Porting Grooves in Positive Displacement Machines: the Case of External Gear Machines

Sidhant Gulati, Andrea Vacca

Maha Fluid Power Research Center, Purdue University, Lafayette, IN, 47905, USA
E-mail: avacca@purdue.edu

Manuel Rigosi

CASAPPA SpA, Via Balestrieri, 1, 43044 Lemignano di Collecchio, Parma (Italy)

Abstract

In all common hydrostatic pumps, compressibility affects the commutation phases of the displacing chambers, as they switch their connection from/to the inlet to/from the outlet port, leading to pressure peaks, localized cavitation, additional port flow fluctuations and volumetric efficiency reduction. In common pumps, these effects are reduced by proper grooves that realizes gradual port area variation in proximity of these transition regions.

This paper presents a method to automatically find the optimal designs of these grooves, taking as reference the case of external gear pumps. The proposed procedure does not assume a specific geometric morphology for the grooves, and it determines the best feasible designs through a multi-objective optimization procedure. A commercial gear pump is used to experimentally demonstrate the potentials of the proposed method, for a particular case aimed at reducing delivery flow oscillations.

KEYWORDS: External gear pumps, design optimization, relief or silencing grooves

1. Introduction

In all positive displacement pumps, the commutations of the displacement chambers (i.e. the tooth space volumes – TSVs – in gear pumps, or the piston–cylinder volumes in piston units) from/to outlet (HP port) to/from inlet (LP port) port is accompanied with undesired compressibility effects. With a proper design of the ports, these chambers are connected to the inlet or to the outlet respectively when their volume increases or decreases. Inevitably, commutations from/to HP and LP ports can be realized only

through gradual port area opening. These regions of partial opening can involve significant variations of the displacing chamber volume, as shown in Fig. 1 for the case of an external gear pump – EGP – (meshing region).

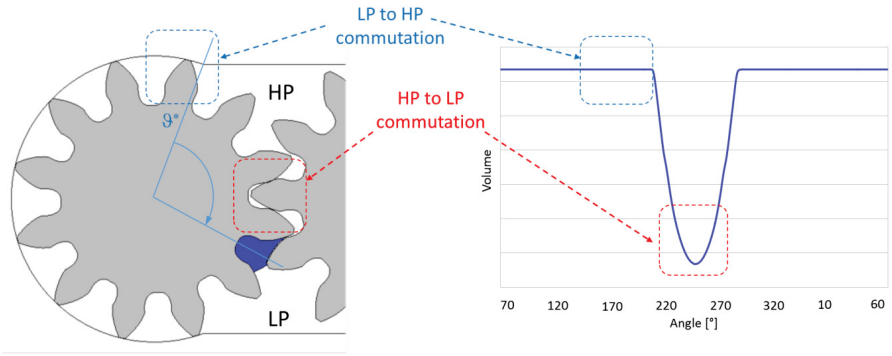

Figure 1 – Instantaneous TSV and IN/OUT commutations in an EGP

These volume variation induces undesired effects: firstly, pressure peaks can arise during the volume decrease with restricted connection to HP. These peaks can be reflected at the outlet port as additional pressure ripples; moreover, in EGP they might affect the radial balance of the gears. Secondly, localized cavitation in the displacement chamber can occur in the region of increasing volume, when the LP connection is gradually opening. Low opening areas in proximity of the min/max volume point can also limit the actual displaced volume, thus affecting volumetric efficiency. Bypass flow from HP to LP can also be established in case of overlap for the port openings (often referred as crossport). This is a condition that can be realized with the aim of increasing the opening area in the region of high volume changes, thus limiting the negative effects described above. All these aspects have been extensively studied in positive displacement machines: /1,2/ represents some of the significant works on EGPs. These past studies highlight the importance of a careful design for the porting areas in the transition phases. Figure 2*a* shows the typical designs of the grooves machined to realize proper porting areas in EGPs. In positive displacement pump designs, these grooves are often referred as “relief grooves” or “silencing grooves”. However, a design procedure able to identify the best geometry morphology for these grooves was never published, and EGP manufacturers often use empirical approaches or simplified numerical procedures according to the designers’ experience. As a consequence, different design morphologies can be found in the market (see Fig. 2b), and no evidence exist to identify which one is more suitable to the pump operation. Some past studies, such as /3/ for EGPs, and /4/ for axial piston pumps, presented optimization procedures for pre-defined geometric morphologies for the port grooves. No published work addresses the problem

of finding the best realizable groove geometry without assuming a shape a priori.

In this paper a numerical optimization procedure is proposed to automatically determine both the optimal porting area and the geometric morphology of the transition grooves. The optimization process consists on a multi-objective genetic algorithm, in which different objective functions are numerically evaluated using a simulation model for EGPs previously developed by the authors' research team /1/. The innovative content of the proposed approach consists in the input parameters used by the optimization process to determine both the areas and the shapes of the grooves. In two separate levels, the procedure determines first the best numerical area function and secondly the most closest realizable shape according to common manufacturing processes.

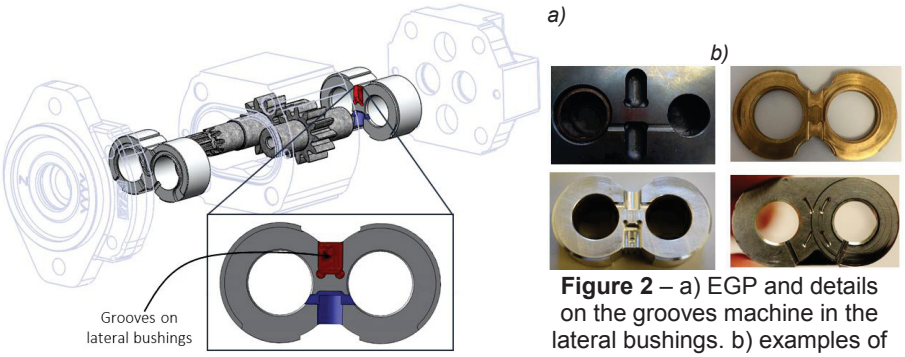

Figure 2 – a) EGP and details on the grooves machine in the lateral bushings. b) examples of typical groove designs

2. Numerical Approach

2.1 Basic EGP simulation

To predict the performance parameters for an EGP with different groove designs, this study benefitted from the tool HYGESim (Hydraulic Gear Machine Simulator) previously developed by the authors' team. As described in /1,5/, HYGESim combines a lumped parameter fluid dynamic model for the analysis of the main flow through the unit with a Fluid Structure Interaction CFD evaluation of the internal lateral gap flow leakages; a mechanical model is then used to evaluate the micro-motions and the balance of the internal pump elements. The lumped parameter model is the main component of HYGESim for this study; according to this model, the TSVs and the inlet/outlet ports are treated as separated control volumes. The pressure in each control volume is then evaluated from continuity eq. /1/:

$$\frac{dp_j}{dt} = \frac{1}{V_j}\frac{dp}{d\rho}\Big|_{p=p_j} \cdot \left[\sum \dot{m}_{in,J} - \sum \dot{m}_{out,J} - \rho|_{p=p_j}\left(\frac{dV_j}{dt} - \frac{dV_{var,j}}{dt}\right)\right] \quad (1)$$

Through an accurate geometrical model that takes the CAD drawings of the gears, the case and the lateral bushings of the pump, the instantaneous volumes as well as the areas of the internal connections between the TSVs and the inlet/outlet port are evaluated by the geometrical model of HYGESim. The connections realized by the grooves in the meshing areas, represented in Fig. 2 are of particular interest for this work. After each TSV is trapped between the points of contact of the gears, these connections are the only openings of the volume to the inlet/outlet ports. In the fluid dynamic model, these connections are treated by using the turbulent orifice equation:

$$\dot{m}_{i,j} = \frac{(p_i - p_j)}{|(p_i - p_j)|} \cdot \rho|_{P=\overline{P_{i,j}}} \cdot \alpha \cdot \Omega_{i,j} \cdot \sqrt{\frac{2 \cdot (p_i - p_j)}{\rho|_{P=\overline{P_{i,j}}}}} \qquad (2)$$

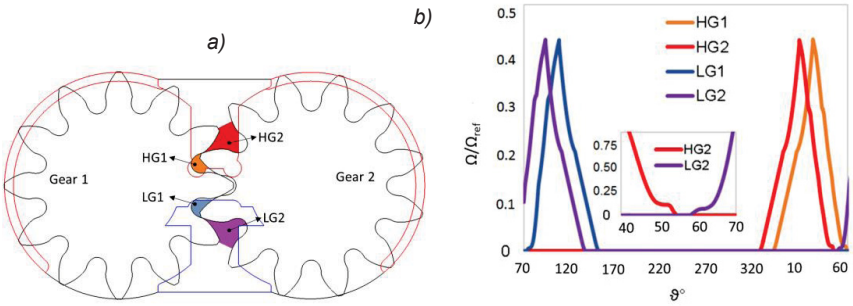

Figure 2 – *a)* the openings realized by the porting grooves in an EGP; *b)* Areas for a reference TSV pair, with the angular convention of Fig. 1

With this approach, HYGESim can estimate parameters characterizing the EGP design such as instantaneous TSV pressure, port pressure fluctuation and volumetric efficiency.

2.2 Optimization Phase I – Area connection realization

The proposed optimization procedure is divided in two phases: Phase I identifies a smooth and realistic groove area (Ω in Eq. 2) curve that guarantees optimum performance of the unit; while in Phase II, a realizable groove shape is found to replicate the optimal area curves obtained from Phase I.

In Phase I, the area profile of each connection is determined by determining the location of a certain number of points of the area function $\Omega = \Omega(\vartheta)$. For the sake of clarity, the procedure is hereafter detailed for the optimization of the HG1 area connection. The area plots for other connections formed by the grooves such as HG2, LG1 and LG2 are optimized in the same fashion. With reference to Fig. 3, the V1 tooth space area curve (in red) represents the projection of the TSV on the lateral side of the gears while the HV1 area curve (in orange) represents the connection area between TSV with the outlet

port though the face width of the gear. After HV1 reaches a null value (for $\vartheta = \vartheta_c \approx 55°$), the TSV on gear 1 is trapped by the point of contact and HG1 is the only connection to the outlet port. HG1 has a primary influence on the pump operation only within the interval $\vartheta_C - \vartheta_{min}$. This because the inlet/outlet commutation of the TSV occurs around $\vartheta = \vartheta_{min} \approx 70°$, and the TSV is open to the outlet port through both HV1 and HG1 before ϑ_c. For this reason, Phase 1 optimizes the location for the HG1 area points only in such region; before ϑ_c, the area of HG1 is simplified by 3 area points as shown in Fig. 3.

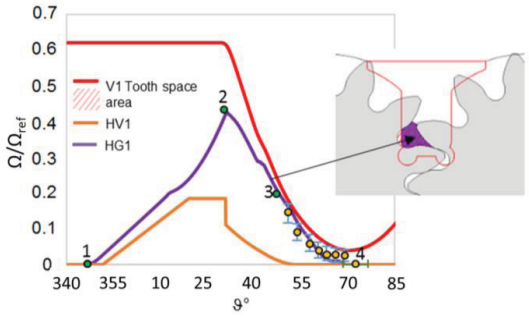

Figure 3 – Area points for the optimization of HG1

These latter points can be initially assumed as points reasonably close to the TSV area curve and are kept fixed during Phase I. The actual HG1 area at these locations will be determined afterwards by Phase II. The yellow points in Fig. 3 are the design input variables provided to the optimizer.

The point 4 in the extreme right represents the angular value at which the HG1 orifice area becomes zero or, in other words, the location at which the HG1 connection closes. The rest of the variable points between the points 3 and 4 are placed with smaller angular interval for the points near the closing of the connection area and larger interval in the remaining region. In this way, more importance is given to the angular region of the groove that realizes minimum opening areas, which is also the region that plays the relevant role during the TSV commutations. For each connection, the number of input points to be optimized during Phase I (in yellow, in Fig. 3), was assumed equal to 8, as best compromise between simulation time and consistency of the results. For the reference pump, a higher number of points does not change significantly the result of the optimization. To generate area input curves to be used as input in the HYGESim simulations, the input points are connected using linear interpolation. It is also important to ensure that these points are explored within a realistic range. For this purpose, if the connection area value is greater than TSV area value at any angular step, the particular design configuration is excluded because unrealistic.

Objective functions (OFs) for Phase I are defined in a similar fashion as in /6/.

1-OF1: Minimize pressure fluctuations: As source of fluid-borne noise and vibrations,

the outlet pressure flow fluctuation should be minimized. As described in /7/, the fluctuations in the flow can be quantified by calculating the energy associated with these signals in the frequency domain:

$$OF_1 = E = \sum_{k=1}^{N} \pi_k \, , where \;\; \pi_k = \sum_{f_k-\Delta f}^{f_k+\Delta f} L(f)^2 \qquad (minimize) \tag{3}$$

In the equation, N here is the number of multiples of the fundamental harmonics considered (typically 5 are enough for the typical shape of the signal), π_k is the total energy of kth harmonic, L(f) is FFT of the pressure ripple signal.

1-OF2: Minimize internal pressure peaks: Pressure overshoots occurring during the meshing process in proximity of the TSV connections need to be minimized in order to reduce noise, mechanical vibrations and instantaneous radial stress to the gears.

1-OF3: Minimize localized cavitation onset: Air release, and in extreme cases vapor cavitation, can occur due to the rapid increase of the TSV volume in the meshing process. This occurs when the TSV pressure falls below the fluid saturation pressure. Therefore, OF3 is defined as the area of the TSV pressure with respect to the rotation angle that falls below the saturation pressure of the fluid:

$$OF_3 = \int P_{TSV} d\theta, \forall \; P_{TSV} < P_{sat} \qquad (minimize) \tag{4}$$

1-OF4: Maximize volumetric efficiency.

2.2 Optimization Phase II – Groove determination

Once the optimal area curves are obtained from Phase I, Phase II solves the problem of determining a feasible – through conventional milling practices - groove shape that would give performance features as close as possible to the optimal area curve. For this purpose, a numerical tool is developed for Phase II to build the groove by the union of basic geometry features such as rectangles, triangles, circles, as shown in Fig. 4*a*. The number of geometrical features (circles, triangles) is selected by the user. Once a groove shape profile is finalized, the HG, LG area connection curves are calculated by using the HYGESim geometric model. A genetic algorithm is then used to find the optimal profile, defined as the one that realizes curves as close as possible to those found by Phase I. Figure 4b shows the inputs required to determine the size and position of each individual geometrical feature utilized during Phase II. The variable positioning of the basic

geometric features, as well as the parameters for the base rectangular shape, permit to study also the implementation of asymmetric grooves, uncommon in commercial EGPs, but potentially convenient in case of asymmetric gear profiles. Phase II is also able to investigate simple shape morphologies, characterized by a number of features lower to the one set by the user. In fact, while performing the union of different features to build the final shape, a feature does not affect the final groove shape if it is placed by the optimizer in such a way that an intersection with the base shape does not exist.

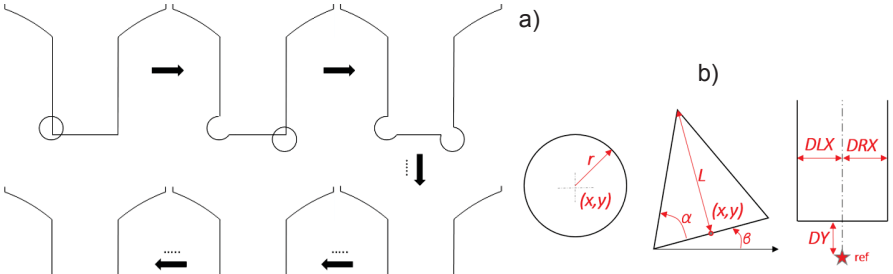

Figure 4 – a) formation of groove shape; b) parameters for the basic geometric primitives

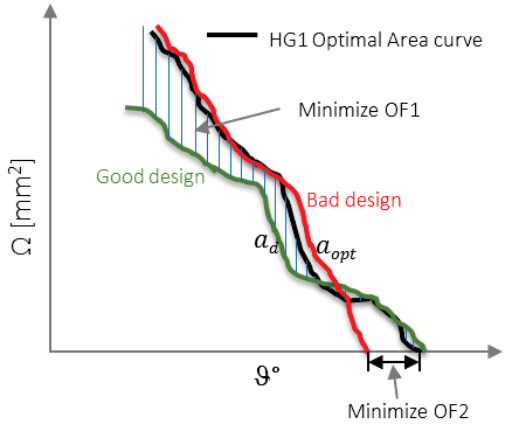

Figure 5 – Objective functions for Phase II

The features related to the delivery grooves are used for the HG1 and HG2 connections, while the suction groove is used for the LG1 and LG2 connections. Therefore, in Phase II the optimization of the delivery groove (for HG1 and HG2 connection areas) can be performed separately from the suction groove (LG1 and LG2).

The OFs for Phase II help in identifying the closest feasible profile to the optimal area curve found in Phase I:

2-OF1: Curve match: This function minimizes the difference between the area curve obtained from the generated groove shape and the optimal connection area defined from Phase I. Figure 5 shows the optimal area curve (from Phase I) in black and two candidate area curves, in red and green. The design in green is considered a better design than the one in red, despite it does not follow the optimal curve in the upstream part. This is

in accordance to what described in section 2.1: regions of small area openings are in proximity of the TSV commutations and therefore have higher importance:

$$OF_1 = abs\left(\frac{a_d - a_{opt}}{a_{opt}}\right) \times P \qquad (minimize) \tag{5}$$

a_d represents the area value for the design generated by the optimization, while a_{opt} represents the optimal value from Phase I. P is a linearly growing ramp to ensure emphasis is given to the region near the meshing process, near the closing/opening.

2-OF2: Opening and closure points: It is of utmost importance to ensure that the porting grooves respect the opening and closing points of the connection as identified by Phase I. This function minimizes the angular difference between the candidate curve and the optimal one in proximity of the opening/closing points (Fig. 5):

$$OF_2 = abs(\theta_{opt} - \theta_d) \qquad (minimize) \tag{6}$$

3. Results and discussion

The proposed numerical optimization procedure was implemented in a modeFrontier® workflow and utilized to design the bushing of a commercial EGP according to the Fast Optimizer algorithm /8/, which combines Response Surface Models to multi-objective evolutionary optimization. To confirm the potential of the procedure, the optimal design found from the optimization was implemented and tested for comparison purposes with the commercial one. The reference pump has a displacement of 22 cm^3/rev and 12 teeth on each gear. A operating condition that falls approximately in the middle of the typical operating range of the reference unit (2000 rpm and p = 0.8*p_{ref} delivery pressure) was considered. Approximately 3500 designs were evaluated during Phase I, for a simulation time of about 3-4 days (using an Intel Core i7-3770 Windows CPU @ 3.40 GHz). From Phase I, a Pareto frontier is obtained between the OFs and the best design is selected from the Pareto optimal region, as best compromise between the five different OFs of Phase I. A subset of the designs evaluated by Phase I, close to the optimal region of the Pareto frontier is plotted using a 4D bubble chart in Fig. 6. In particular, the pressure pulsations at outlet and TS pressure overshoot are plotted on x axis and y axis respectively, the color of bubble represents the volumetric efficiency and the diameter of bubble gives an estimate of the cavitation. This graph helps in understanding the tradeoff between OFs and their dependence on different groove profile designs. From Fig. 6 it is interesting to observe how the groove profiles for the reference pump fall in the optimal region, indicating how there is no much margin of improvement for the reference unit.

However, with the aim of further reducing the level of outlet pressure fluctuation, a design with higher pressure peak was chosen for further consideration.

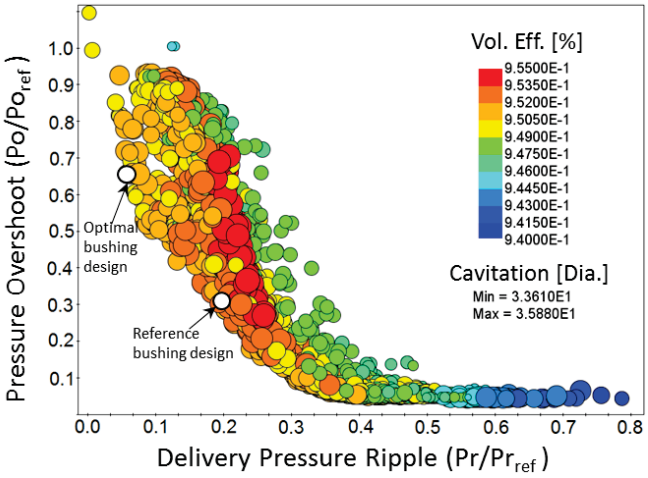

Figure 6 - Pareto frontier between TSV pressure overshoot and delivery pressure ripple. Vol. efficiency and localized cavitation OFs are also reported (all values normalized).

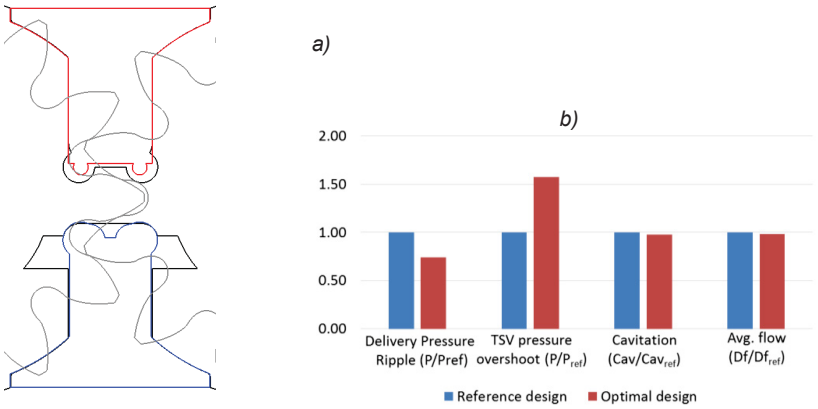

Figure 7 – a) Groove showing the superposition of selected optimal design over the reference design; b) comparison between OFs for the optimal and reference design

Phase II was executed afterwards to find an actual shape for the optimal grooves. Around 5,000 designs were evaluated, for about two days of computational time (same computer specified above). Figure 7a shows the original profile (in black) of the grooves superimposed with those found by the proposed procedure (in red and blue respectively) The optimal delivery groove is formed by a base rectangle and circle, while the optimal suction groove is formed by a base rectangle and two circles. Because of the nature of the design of the reference pump (symmetric teeth, with minimum backslash in the meshing zone), no significant asymmetry appears in the optimal grooves. Also, in the

Pareto frontier of the best designs for Phase II, it was possible to identify a design without triangular features, thus of easier realization.

The performance of the new optimal design in terms of OFs was compared against the baseline unit through HYGESim simulations and compared with the predictions performance of the baseline design, Fig. 7b (normalized OFs). The delivery pressure ripple in the simulation is reduced by 26%, with an increment of the pressure overshoot of about 1.5 times. The other OFs are marginally affected with the new grooves.

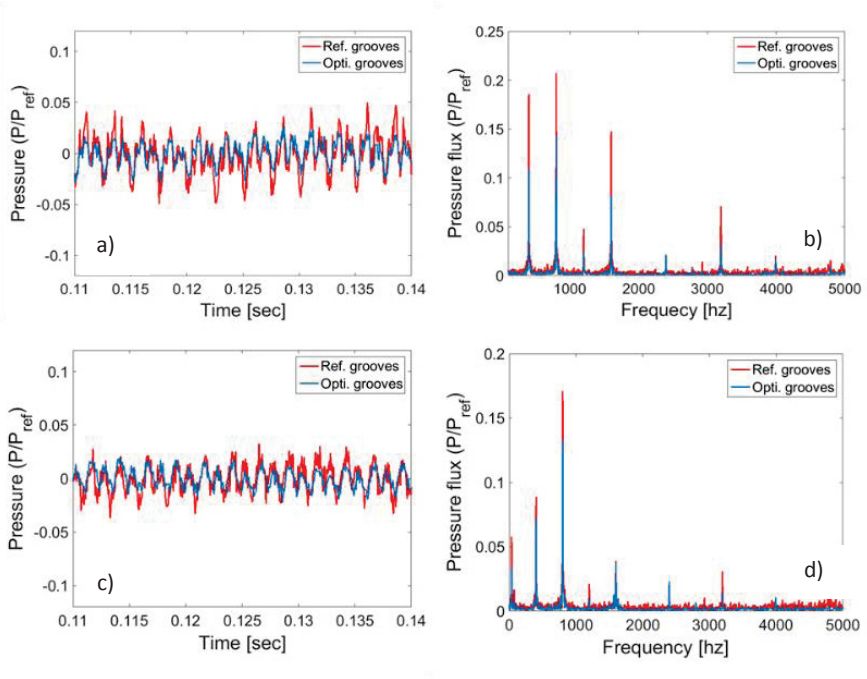

Figure 8 - Experimental outlet pressure ripple for the reference EGP, using the standard grooves (red) and the optimized ones (blue) at n = 2000 rpm: (a) time signal at p/p_{ref} =0.8, (b) FFT signal at p/p_{ref} =0.8, (c) time signal at p/p_{ref} = 0.4; (d) FFT at p/p_{ref} = 0.4

To validate the performance of the new design obtained from the proposed numerical procedure, experiments were performed at the Maha Fluid Power Research Center of Purdue University. The experiments for both reference and optimal bushing were performed using the baseline pump with same gears but replacing the lateral bushings. The hydraulic circuit used for the tests is in accordance with the ISO 4409 standards for pump characterization. Piezoelectric pressure sensors are flush mounted in a calibrated (easy to reproduce in a simulation environment) outlet rigid pipe used to measure the outlet pressure pulsations, as described in /7/. In Fig. 8, the experimental results are shown for two different operating conditions, i.e. 2000 rpm and 1500 rpm at p/p_{ref} = 0.8.

The difference in the pressure ripple can entirely be accounted due to the change in the profile of the grooves because all other factors affecting the pressure signal including the pump is kept same in the experiment. It can be observed that optimal grooves show a smaller pressure ripple magnitude than the reference ones for both the operating conditions. This trend can also be seen over the range of frequencies in the plots showing the FFT of the signal. The optimal groove design shows lower amplitude of peaks and thus lower energy in the pressure signal as compared to reference groove design.

4. Conclusions

The paper presented a novel methodology to optimize the profile of the porting grooves which affects the behavior of pumps during the HP/LP commutations of the internal displacement chambers, particularly as concerns fluid borne noise, volumetric efficiency, occurrence of cavitation and of internal pressure peaks. This paper particularly refers to the case of external gear machines, for which a simulation model (HYGESim) is available at the authors' research center to study the effects of the porting grooves at the lateral side of the gears with high level of details.

The proposed optimization methodology consists of two phases: in the first phase (Phase I), the optimal area of the connections for each displacing chamber with the inlet/outlet port is defined. Phase I does not assume a particular geometrical morphology for the porting groove: it simply optimizes proper points of the function area vs. shaft position. In the second phase (Phase II), the best groove shape is found by an algorithm that combines basic parametric geometric features (rectangle, circle, triangle) to identify the best actual geometry able to match the result found in Phase I. The novelty of the proposed procedure consists in its generality: in fact, the procedure does not assume any specific geometric template to optimize and thus can permit more freedom in allowing unconditional groove profiles.

To show the potentials of the proposed algorithm, the case of a commercial 22 cm^3/rev pump was considered. The optimization procedure permitted to confirm that the commercial design used by the manufacturer is already close to the optimum, according to the objective functions (OFs) considered in the research. Despite this observation, it another design lying on the optimal Pareto frontier, characterized by a different compromise between the OFs that decreases outlet pressure ripples, was tested. Both simulation results and experiments confirmed the results anticipated by the procedure, showing a reduction of the pressure ripple in the order of 30%, obtained by accepting larger pressure peaks associated with the meshing process of the pump.

5. Acknowledgement:

The authors would like to thank Esteco, for the use of the optimization software modeFrontier®, and Siemens, for the software AMESim® used to perform the simulation with HYGESim.

6. References

/1/ Vacca A., Guidetti M., 2011, Modelling and Experimental Validation of External Spur Gear Machines for Fluid Power Applications, Simulation Modelling Practice and Theory 19.9 (2011): 2007-2031.

/2/ Eaton M., Keogh P.S., Edge K.A., 2006, The Modelling, Prediction, and Experimental Evaluation of Gear Pump Meshing Pressure with Particular Reference to Aero-Engine Fuel Pumps, in: Proc. IMechE, Part I: Systems and Control Engineering (vol. 220), 2006

/3/ Wang S., Sakurai H., Kasarekar A., 2011, The Optimal Design in External Gear Pumps and Motors, Mechatronics, IEEE/ASME Transactions on Mechatronics, 16.5 (2011): 945-952

/4/ Seeniraj G., Ivantysynova M., 2011, A Multi-Parameter Multi-Objective Approach to Reduce Pump Noise Generation. International Journal of Fluid Power, Vol. 12, No. 1, pp. 7 - 17.

/5/ Dhar S., Vacca A., 2013, A Fluid Structure Interaction—EHD Model of the Lubricating Gaps in External Gear Machines: Formulation and Validation, Tribology International 62 (2013): 78-90

/6/ Devendran R.S., Vacca A., 2013, Optimal Design of Gear Pumps for Exhaust Gas Aftertreatment Applications, Simulation Modelling Practice and Theory, vol. 38 (2013): 1-19

/7/ Vacca A., Franzoni G., Casoli P., 2007, On the Analysis of Experimental Data for External Gear Machines and their Comparison with Simulation Results, IMECE2007 ASME International Mechanical Engineering Congress and Exposition, November 11-15, 2007, Seattle,USA

/8/ Deb K., Pratap A., Agarwal S., Meyarivan T., 2002, A Fast and Elitist Multiobjective Genetic Algorithm: NSGA-II, Evolutionary Computation, IEEE Transactions on 6.2 (2002): 182-197.